Progress In Electromagnetics Research M, Vol. 50, 129–140, 2016

A New MIMO Channel Model Incorporating Antenna Effects

Qiuming Zhu*, Cuiwei Xue, Xiaomin Chen, and Ying Yang

Abstract—Antenna characteristics including mutual coupling and polarization/depolarization have great effects on the performance of Multiple-input multiple-output (MIMO) system. In this paper, new close-form expressions of signal vector, signal power and signal correlation incorporating mutual coupling and polarization/depolarization are derived firstly. On this basis, we present a new MIMO channel model, which takes into account antenna effects such as mutual coupling and antenna polarization, as well as propagation effects such as scattering, clustering and channel depolarization. In particular, the detailed expressions of a 2×2 MIMO channel considering mutual coupling and polarization configurations of slanted $\pm 45^\circ$ and V/H are derived. Finally, these expressions are applied to the propagation scene of suburban macro cellular to analyze the channel correlation and capacity, which is very helpful in designing and optimizing a MIMO system.

1. INTRODUCTION

Multiple-input multiple-output (MIMO) systems, where multiple antennas are used at both transmitter and receiver, are expected to play a key role in improving the capacity of wireless communication systems. However, insufficient antenna spacing and lack of scatterings will reduce capacity due to the increased channel correlation [1]. Moreover, when antennas are placed close to one another, mutual coupling (MC) could not be negligible, which will affect channel correlation significantly [2]. In [3], a deeper understanding of MC mechanism between antennas was given and a MC matrix had also been derived in particular. Wu and Bergmans in [4] presented a MIMO channel matrix considering MC, and studied the effects of MC on spatial correlation. The channel capacity of MIMO channel was simulated to study the significance of MC effects, which shows that capacity can be increased by properly incorporating coupling in [5].

On the other hand, polarized antennas can offer a much better separation between channels, which draws ever more attention in the design of diversity systems, as well as MIMO systems [6]. MIMO systems where multipath fading is only partially correlated could use polarization diversity to provide a higher diversity gain. In the fading environment, the performance of a MIMO diversity system is improved [7], and the capacity gain can be obtained through polarization diversity [8]. As to polarization diversity, [9] had discussed possible effects of different spatial correlation coefficients and average power ratios due to different antenna array structures on the diversity gain. The polarized MIMO channel model including 2D and 3D, was provided in detail, which took into account both azimuth and elevation spectrum for different environments in [10]. Manh-Tuan Dao [11] proposed a new 3D polarized geometry model and derived a close-form expression of spatial correlation, including both arbitrary antenna structure and 3D propagation environment. A analytical upper bound and lower bound on the ergodic capacity of polarized distributed antenna system and its relation with polarization effect are discussed in [12]. Joung et al. [13] analyzed the effects of polarization mismatch and space-correlation to a

Received 28 July 2016, Accepted 14 September 2016, Scheduled 27 September 2016

* Corresponding author: Qiuming Zhu (zhuqiuming@nuaa.edu.cn).

The authors are with the College of Electronic and Information Engineering, Nanjing University of Aeronautics and Astronautics, Nanjing 211106, China.

multiple-input and single output (MISO) channel, and found that polarization mismatch decreases the ergodic capacity by degrading signal power, whereas space-correlation does this by reducing diversity gain.

Therefore, the effects of antenna array including spacing, pattern, orientation and polarization should be taken into account to evaluate the performance of MIMO systems [14, 15]. In this paper, the mechanism of MC and polarization is studied in detail, and on this basis the power and spatial correlation expressions of MC and polarization are derived. Finally, a new MIMO channel matrix and spatial correlation expression combining MC with polarization are given.

The paper is arranged as follows. Section 2 presents a system model of MIMO channel and derives expressions of power and spatial correlation. Section 3 analyzes the effect of antenna configurations which contains MC and polarization. Simulation results of spatial correlation and channel capacity of 2×2 MIMO channel with different antenna configurations are presented in Section 4. Finally, conclusions are drawn in Section 5.

2. SYSTEM MODEL

We consider an MIMO system with M_t transmitting antennas and M_r receiving antennas, where scatterers around the antenna arrays are grouped into clusters as shown in Fig. 1. The location of clusters on transmitter and receiver sides is defined by mean angle of departure (AoD) and mean angle of arrival (AoA) respectively. v_r, θ_r^v and v_t, θ_t^v are moving speed and direction of receiver and transmitter sides.

The ray-based clustered approach is widely used to model MIMO channels [16], which has also been adopted by WINNER channel model, 3GPP SCM, and IEEE 802.11n channel model. Using the clustered channel model, the wide-band channel response matrix is given as

$$\hat{\mathbf{H}}(t,\tau) = \sum_{l=1}^{L} \mathbf{H}_l(t)\boldsymbol{\delta}(\tau - \tau_l) \tag{1}$$

where $\mathbf{H}_l(t)$ is the channel matrix caused by the lth cluster of scatterers or the channel corresponding

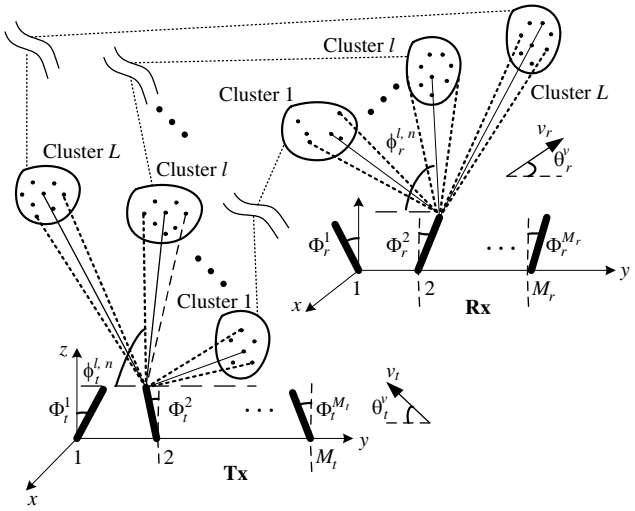

Figure 1. Clustered MIMO channel.

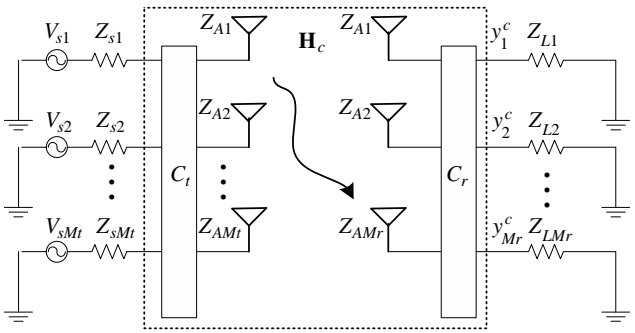

Figure 2. Equivalent $M_t \times M_r$ MIMO channel with mutual coupling.

to the lth cluster. $\mathbf{H}_l(t)$ can be further represented by a normalized sum of sub-rays within the cluster,

$$[\mathbf{H}_l]_{M_r\times M_t} = \iint_{\left\{\phi_r^l,\,\phi_t^l\right\}} e^{j2\pi f_c t} e^{j2\pi f_c \frac{v_t\cos\left(\phi_t^l-\theta_t^v\right)+v_r\cos\left(\phi_r^l-\theta_r^v\right)}{c}t} p\left(\phi_r^l\right) p\left(\phi_t^l\right) \odot\left\{\mathbf{y}_r\left(\phi_r^l\right)\left(\mathbf{y}_t\left(\phi_t^l\right)\right)^T\right\} d\phi_r^l d\phi_t^l \tag{2}$$

Here, AoD and AoA within the lth cluster are denoted as ϕ_t^l and ϕ_r^l. $p(\phi_r^l)$ and $p(\phi_t^l)$ denote the probability distribution function (PDF) of AoA and AoD, respectively. In this paper, we only consider flat fading channel. $\mathbf{y}_t(\phi_t)$ and $\mathbf{y}_r(\phi_r)$ are the signal vectors of transmitter and receiver, which can be expressed as

$$\mathbf{y}_{t/r}^{nc}\left(\phi_{t/r}\right) = \mathbf{g}^{nc}\left(\phi_{t/r}\right)\cdot\mathbf{a}\left(\phi_{t/r}\right) \tag{3}$$

where $\mathbf{g}^{nc}(\phi_{t/r})$ is the antenna gain and $\mathbf{a}(\phi_{t/r})$ the antenna steering vector. In the following, we take an example of receiver side due to the symmetry of two sides. Then the power of kth receiving signal can be calculated by

$$P_k^{nc} = \int_{\{\phi_r\}} \left|g_k^{nc}(\phi_r)a_k(\phi_r)\right|^2 p(\phi_r)d\phi_r \tag{4}$$

The definition of spatial correlation coefficient, also known as cross-correlation coefficient, between antenna k and q can be expressed as

$$\rho_{k,q}^{nc} = \frac{1}{\sqrt{P_k^{nc}P_q^{nc}}}\int_{\{\phi_r\}} y_k^{nc}(\phi_r)\left(y_q^{nc}(\phi_r)\right)^* p(\phi_r)d\phi_r \tag{5}$$

3. ANTENNA EFFECTS ON SIGNAL AND CHANNEL

3.1. Impact of Mutual Coupling

Mutual coupling describes the electromagnetic interaction among multiple antenna elements. When antenna elements are very close, the field generated by one antenna will alter the current distributions of others. In this way, radiation pattern and input impedance of each element are disturbed by the presence of other elements, which is similar with signal crosstalk in circuit system. The $M_t\times M_r$ equivalent MIMO channel model with MC is presented in Fig. 2. $V_{s1}, V_{s2}, \ldots, V_{sM_t}$ are voltage values of transmitting antennas, and $Z_{s1}, Z_{s2}, \ldots, Z_{sM_t}$ are source impedances. $Z_{A1}, Z_{A2}, \ldots, Z_{AM_t}$ and $Z_{A1}, Z_{A2}, \ldots, Z_{AM_r}$ are antenna impedances of transmitter and receiver, respectively. $Z_{L1}, Z_{L2}, \ldots, Z_{LM_r}$ are load impedances.

Taking receiver as an example, the equivalent voltage of antennas can be obtained according to circuit theory. Assuming load impedance, antenna impedance and source impedance of each branch being equivalent, $\mathbf{C}_r$ can be deduced as

$$\mathbf{C}_r = \left(Z_L + Z_A\right)\left(\mathbf{Z}_L + \mathbf{Z}_r\right)^{-1} \tag{6}$$

where $\mathbf{Z}_L$, $\mathbf{Z}_r$ are load impedance matrix and mutual impedance matrix. Similarly, the coupling matrix of transmitting side can be derived as

$$\mathbf{C}_t = \left(Z_S + Z_A\right)\left(\mathbf{Z}_S + \mathbf{Z}_t\right)^{-1} \tag{7}$$

Here $\mathbf{Z}_S, \mathbf{Z}_t$ are source impedance matrix and mutual impedance matrix of transmitter, and the elements of mutual impedance matrix can be calculated by [14]

$$Z_{kq} = \begin{cases} 30\left[0.577 + \ln(2\pi) - \mathrm{Ci}(2\pi) + \mathrm{jSi}(2\pi)\right], & k = q \\ 30\left[2\mathrm{Ci}(2\pi/\lambda d_{k,q}) - \mathrm{Ci}\left(2\pi/\lambda\left(\sqrt{d_{k,q}^2 + {L_A}^2} + L_A\right)\right) - \mathrm{Ci}\left(2\pi/\lambda\left(\sqrt{d_{k,q}^2 + {L_A}^2} - L_A\right)\right)\right] & \\ -30\mathrm{j}\Bigg[2\mathrm{Si}(2\pi/\lambda d_{k,q}) - \mathrm{Si}\left(2\pi/\lambda\left(\sqrt{d_{k,q}^2 + {L_A}^2} + L_A\right)\right) & \\ -\mathrm{Si}\left(2\pi/\lambda\left(\sqrt{d_{k,q}^2 + {L_A}^2} - L_A\right)\right)\Bigg], & k \neq q \end{cases} \tag{8}$$

where L_A is the antenna length, and $d_{k,q}$ is the distance between antennas k and q. $C_i(x)$ and $S_i(x)$ denote cosine and sine integrals functions. In the presence of mutual coupling, signal vectors for both transmitter and receiver should be revised as

$$\mathbf{y}_{t/r}^{c}\left(\phi_{t/r}\right)=\mathbf{C}_{t/r}\cdot\mathbf{y}_{t/r}^{nc}\left(\phi_{t/r}\right) \tag{9}$$

Taking receiver as an example, MC will make the signal of kth antenna to be a weighted summation of all branch signals, and the weighting coefficients are the corresponding line of coupling matrix. Using two half-wave dipole and omnidirectional antennas as an example, the magnitude of signal including MC for several inter-element distances is given as Fig. 3. Here, the self-impedance is calculated by Eq. (8) for the case of $k=q$, which is $z_A=(73+42.5\mathrm{j})\Omega$, and the load impedance is assumed to match to self-impedance, $z_L=(73-42.5\mathrm{j})\Omega$. The received signal vector without coupling effects is also showed in Fig. 3 for comparison. As we can see, MC will cause a distortion, which is related to the inter-element distance. The distortion is not appreciable when $d>\lambda$, but it will be significant as d decreases. For the 3rd generation (3G) mobile system, the radio wave length is about a few tens of centimeters, so it is very difficult to avoid the effects of MC. In addition, the signal on antenna 1 is symmetrical to that on antenna 2, which is the consequence of MC matrix's symmetry.

Submitting Eq. (9) into Eq. (4), the received power with MC should be revised as

$$P_k^c=\sum_{n=1}^{M_r}C_{kn}C_{kn}^{*}+\sum_{n=1}^{M_r}\sum_{m=1,\,m\neq n}^{M_r}C_{kn}C_{km}^{*}\rho_{n,m}^{nc} \tag{10}$$

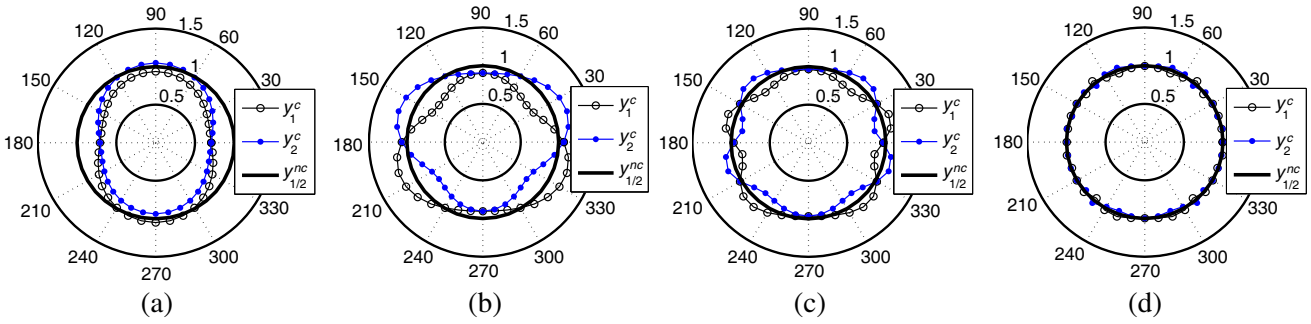

Figure 3. Magnitude of signal vectors incorporating mutual coupling. (a) $d=0.15\lambda$, (b) $d=0.5\lambda$, (c) $d=1\lambda$, (d) $d=3\lambda$.

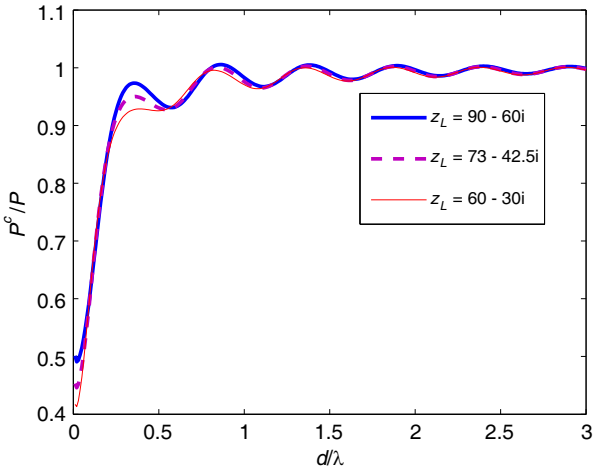

Figure 4. Ratio of total power including coupling.

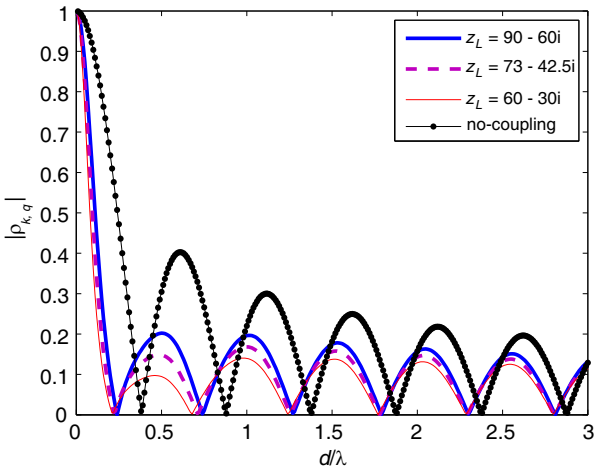

Figure 5. Magnitude of cross-correlation coefficient including coupling.

where $\rho_{n,m}^{nc}$ denotes the correlation coefficient between antennas m and n without MC. Thus, the total received power can be rewritten as $P_{sum}^{c} = P_1^c + P_2^c + \ldots + P_{M_{t/r}}^c$. Similarly, the modified correlation coefficient incorporating with MC can be derived as

$$\rho_{k,q}^{c} = \frac{1}{\sqrt{P_k^c P_q^c}} \left\{ \sum_{n=1}^{M_r} C_{kn} C_{qn}^{*} + \sum_{n=1}^{M_r} \sum_{m=1,\, m\neq n}^{M_r} C_{kn} C_{qm}^{*} \rho_{n,m}^{nc} \right\} \tag{11}$$

Under the same simulation parameters of Fig. 3, the ratio of total power between considering MC and neglecting MC is given in Fig. 4. Here, we assume AoA following uniform distribution over $[0,\ 2\pi)$. As we can see, the power loss is significant and decreases with the increase of inter-element distance, when d/λ is less than 0.5. If d/λ is larger than 0.5, the loss tends to be zero, and it fluctuates slightly between 0.97 and 1. We also find that the power loss is almost the same for different load impedances. The magnitude of cross-correlation coefficients between two receiving antennas with different d/λ is calculated by (11) and shown in Fig. 5. For comparison purpose, the theoretical cross-correlation coefficient in absence of MC can derived from (5). As seen in Fig. 5, all correlation coefficient curves decrease rapidly when inter-element distance increases, and the existence of MC will reduce the correlation. Moreover, different load impedances have different effects on each curve, but the curves tend to be same as d/λ increases.

3.2. Impact of Polarized Antennas

The polarization effect including antenna polarization response and channel depolarization is of great significance for polarized MIMO channel. As to antenna polarization response, we can decompose the polarization into vertical and horizontal directions. Moreover, while the horizontal components tend to mix with each other strongly, the mixture between horizontal and vertical components is relatively small, with a path cross-polar discrimination (XPD) ratio typical larger than 6 dB. Therefore, we need to model four channels between transmitter and receiver, namely those connecting the horizontal/vertical polarization on transmitter to the horizontal/vertical polarization on receiver, which results in the decomposition of antenna patterns at both ends into vertical and horizontal.

Due to the consistency of transmitter and receiver, a 3D polarization antenna model on receiver with polarization angle Φ_r is given in Fig. 6. In the figure, xyz and $x'y'z'$ are geographic coordinate system (GCS) and element coordinate system (ECS). $\hat{\theta}_r$ and $\hat{\phi}$ denote vertical polarization direction and horizontal polarization direction. Both of them are perpendicular to $\vec{k}$, which is the propagation direction of electromagnetic wave. The full response vector of polarized antenna, denoted as $\vec{p}$, includes vertical component and horizontal component which can be obtained by expressing $\vec{p}$ in θ_r and ϕ_r direction. In order to facilitate the research, we use GCS to show vector $\vec{p}$ and $\hat{\theta}_r$, which are

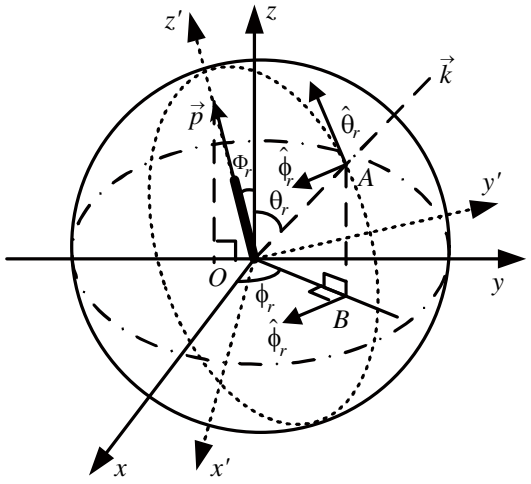

Figure 6. 3D polarization antenna model.

$(0, -\sin\Phi_r, \cos\Phi_r)$ and $(-\cos\theta_r\cos\phi_r, -\cos\theta_r\sin\phi_r, \sin\theta_r)$ respectively. Vector $\hat{\phi}_r$ is perpendicular to $\vec{k}$, and also perpendicular to vector $\hat{\theta}_r$, so vector $\hat{\phi}_r$ is perpendicular to plan oAB. Move vector $\hat{\phi}_r$ to xoy, it is also perpendicular to oB and can be expressed as $(\sin\phi_r, -\cos\phi_r, 0)$. Thus, we obtain $b_r^V(\vec{p}\cdot\hat{\theta}_r)$ and $b_r^H(\vec{p}\cdot\hat{\phi}_r)$, which are 3D polarization antenna response as

$$\begin{bmatrix} b_r^V \\ b_r^H \end{bmatrix} = \begin{bmatrix} \cos\Phi_r\sin\theta_r + \sin\Phi_r\cos\theta_r\sin\phi_r \\ \sin\Phi_r\cos\phi_r \end{bmatrix} \tag{12}$$

For the special case of 2D model ($\theta_r = \pi/2$, $\hat{\theta}_r = (0,0,1)$), b_r^V is equal to $\cos\Phi_r$ while b_r^H is equal to $\sin\Phi_r\cos\phi_r$. Due to the effect of scatterers, the characteristics of polarized radio will be changed during propagation. The scattering effect can be expressed by channel depolarization matrix, which is

$$\mathbf{S} = \begin{bmatrix} h_{VV} & h_{VH} \\ h_{HV} & h_{HH} \end{bmatrix} = \begin{bmatrix} e^{j\varphi^{VV}} & \sqrt{1/\mathrm{XPD}}e^{j\varphi^{VH}} \\ \sqrt{1/\mathrm{XPD}}e^{j\varphi^{HV}} & e^{j\varphi^{HH}} \end{bmatrix} \tag{13}$$

where $e^{j\varphi^{VV}}$, $e^{j\varphi^{VH}}$, $e^{j\varphi^{HV}}$, $e^{j\varphi^{HH}}$ are random phases and follow uniform distribution over $[-\pi, \pi]$. XPD is the ratio of receiving power from co-polarized and cross-polarized channels, which is equal to $|h_{VV}|^2/|h_{HV}|^2$. The higher the XPD is, the less energy is coupled to cross-polarized channel. Results of field test show that XPD is usually a random variable following lognormal distribution, with the mean and variance of 8 dB in urban environment [10]. For a $M_t \times M_r$ MIMO system, the signal vectors on transmitter and receiver can be rewritten as

$$\mathbf{y}_{t/r}^p = \begin{bmatrix} \cos\Phi_{t/r}^1 g_{t/r}^1 a_{t/r}^1 & \sin\Phi_{t/r}^1\cos\phi_{t/r} g_{t/r}^1 a_{t/r}^1 \\ \cos\Phi_{t/r}^2 g_{t/r}^2 a_{t/r}^2 & \sin\Phi_{t/r}^2\cos\phi_{t/r} g_{t/r}^2 a_{t/r}^2 \\ \vdots & \vdots \\ \cos\Phi_{t/r}^{M_{t/r}} g_{t/r}^{M_{t/r}} a_{t/r}^{M_{t/r}} & \sin\Phi_{t/r}^{M_{t/r}}\cos\phi_{t/r} g_{t/r}^{M_{t/r}} a_{t/r}^{M_{t/r}} \end{bmatrix} \tag{14}$$

and the power of kth signal including polarization effect can be expressed as

$$\begin{aligned} P_k^p \;=\; & \left|\cos\Phi_r^k\right|^2 \int_{\{\phi_r\}} y_k^{nc}(\phi_r)(y_k^{nc}(\phi_r))^* p(\phi_r) d\phi_r \\ & + |\sin\Phi_r^k|^2 \int_{\{\phi_r\}} \cos\phi_r(\cos\phi_r)^* y_k^{nc}(\phi_r)(y_k^{nc}(\phi_r))^* p(\phi_r) d\phi_r \end{aligned} \tag{15}$$

Making use of (14) and (15), the cross-correlation coefficient can be revised as

$$\begin{aligned} \rho_{k,q}^p \;=\; & \cos\Phi_r^k(\cos\Phi_r^q)^* \Big/ \sqrt{P_k^p P_q^p} \int_{\{\phi_r\}} y_k^{nc}(\phi_r)\big(y_q^{nc}(\phi_r)\big)^* p(\phi_r) d\phi_r \\ & + \sin\Phi_r^k(\sin\Phi_r^q)^* \Big/ \sqrt{P_k^p P_q^p} \int_{\{\phi_r\}} \cos\phi_r(\cos\phi_r)^* y_k^{nc}(\phi_r)\big(y_q^{nc}(\phi_r)\big)^* p(\phi_r) d\phi_r \end{aligned} \tag{16}$$

Figure 7 gives the normalized power on polarized antenna with different polarization angles. As we can see, the value is 1 when Φ_r^k is equal to 0°, which is equal to the case of no polarization, and it decreases when polarization angle changes away from 0°. In order to compare correlation properties between different antenna configurations, three pairs of polarization angle (0°/0°, 45°/−45° and 0°/90°) are adopted for simulation, and AOA is assumed to follow uniform distribution. Simulation results is given in Fig. 8, which show that for the case of 0°/0°, cross-correlation is equal to the case of no polarization effect. The cross-correlation of $45°/-45°$ combination decreases in comparison to 0°/0°. Particularly, when 0°/90° combination is used, the cross-correlation coefficient is minimum and close to zero.

3.3. Proposed MIMO Channel Model

Based on the above analysis, the MIMO channel with MC can be expressed by

$$[\mathbf{H}^c]_{M_r\times M_t} = \iint_{(\phi_r,\phi_t)} \left\{ e^{j2\pi f_c t} e^{j2\pi f_d t} p(\phi_r) p(\phi_t) \right\} \odot \left\{ \mathbf{C}_r \left\{ \mathbf{y}_r^{nc}(\phi_r)(\mathbf{y}_t^{nc}(\phi_t))^T \right\} \mathbf{C}_t \right\} d\phi_t d\phi_r \tag{17}$$

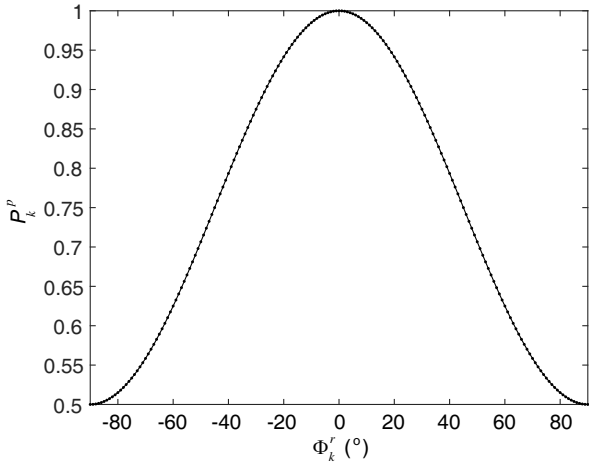

Figure 7. Power loss of single antenna versus polarization angle.

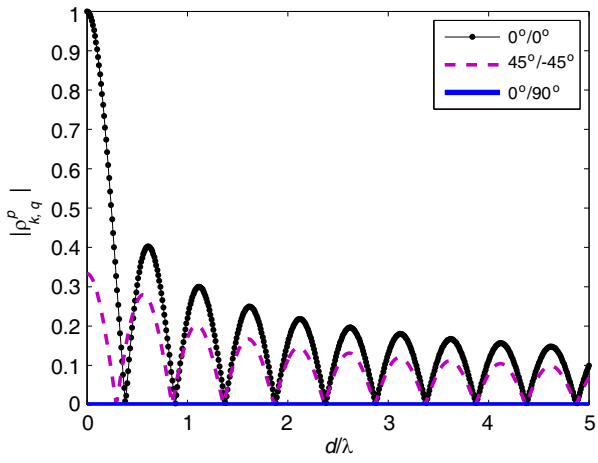

Figure 8. Magnitude of cross-correlation coefficient including polarization.

where $\mathbf{y}_{t/r}^{nc}(\phi_{t/r})$ are shown in Eq. (3) and f_d is equal to $f_c(v_t\cos(\phi_t^l-\theta_t^v)+v_r\cos(\phi_r^l-\theta_r^v))/c$. On the other hand, the MIMO channel with polarization can be modeled as

$$[\mathbf{H}^p]_{M_r\times M_t}=\iint_{(\phi_r,\phi_t)}\left\{e^{j2\pi f_c t}e^{j2\pi f_d t}p(\phi_r)p(\phi_t)\right\}\odot\left\{\mathbf{y}_t^p(\phi_t)\begin{bmatrix}h_{VV} & h_{VH}\\ h_{HV} & h_{HH}\end{bmatrix}(\mathbf{y}_r^p(\phi_r))^T\right\}^T d\phi_t d\phi_r \quad (18)$$

here $\mathbf{y}_t^p$ and $\mathbf{y}_r^p$ are given as Eq. (14). Combining Eqs. (17) and (18), we can get the proposed MIMO channel model incorporating both MC and polarization, which is

$$[\mathbf{H}^{p,c}]_{M_r\times M_t}=\iint_{(\phi_r,\phi_t)}\mathbf{Q}\odot\left\{e^{j2\pi f_c t}e^{j2\pi f_d t}p(\phi_r)p(\phi_t)\right\}\odot\left\{\mathbf{C}_r\left\{\mathbf{y}_r^{nc}(\phi_r)(\mathbf{y}_t^{nc}(\phi_t))^T\right\}\mathbf{C}_t\right\}d\phi_t d\phi_r \quad (19)$$

where

$$\mathbf{Q}=\left\{\begin{bmatrix}\cos\Phi_t^1 & \sin\Phi_t^1\cos\phi_t\\ \cos\Phi_t^2 & \sin\Phi_t^2\cos\phi_t\\ \vdots & \vdots\\ \cos\Phi_t^{M_t} & \sin\Phi_t^{M_t}\cos\phi_t\end{bmatrix}\begin{bmatrix}h_{VV} & h_{VH}\\ h_{HV} & h_{HH}\end{bmatrix}\begin{bmatrix}\cos\Phi_r^1 & \sin\Phi_r^1\cos\phi_r\\ \cos\Phi_r^2 & \sin\Phi_r^2\cos\phi_r\\ \vdots & \vdots\\ \cos\Phi_r^{M_r} & \sin\Phi_r^{M_r}\cos\phi_r\end{bmatrix}\right\}^T \quad (20)$$

According to the definition of channel correlation matrix, including the factors of transmitter, channel and receiver, the channel correlation between $h_{i,p}^{p,c}$ and $h_{j,q}^{p,c}$ can be derived as

$$\begin{aligned}\rho_{i,p;\,j,q}^{h,p,c} &= \iint_{(\phi_r,\phi_t)}\left[\mathbf{Q}\odot\left\{\mathbf{C}_r\left(\mathbf{y}_r^{nc}(\phi_r)(\mathbf{y}_t^{nc}(\phi_t))^T\right)\mathbf{C}_t\right\}\right]_{i,p}\\ &\quad\left[\mathbf{Q}\odot\left\{\mathbf{C}_r\left(\mathbf{y}_r^{nc}(\phi_r)(\mathbf{y}_t^{nc}(\phi_t))^T\right)\mathbf{C}_t\right\}\right]_{j,q}^*p(\phi_r)p(\phi_t)d\phi_t d\phi_r \end{aligned}\quad (21)$$

4. SIMULATION AND APPLICATION

4.1. 2 × 2 Channel Model

As an example, we consider a 2 × 2 MIMO system with half-wave dipole omnidirectional antennas which has $\Phi_t^1/\Phi_t^2=45°/-45°$, $\Phi_r^1/\Phi_r^2=0°/90°$, and the antenna spacing is the same and equal to d. According to Eq. (19), this channel including both polarization and MC can be derived as

$$[\mathbf{H}^{p,c}]_{2\times 2}=\iint_{(\phi_r,\phi_t)}\left\{e^{j2\pi f_c t}e^{j2\pi f_d t}p(\phi_r)p(\phi_t)\right\}\odot\left\{\mathbf{Q}\odot\left\{\mathbf{C}_r\begin{bmatrix}1 & e^{j\tau_t}\\ e^{j\tau_r} & e^{j\tau_r}e^{j\tau_t}\end{bmatrix}\mathbf{C}_t\right\}\right\}d\phi_t d\phi_r \quad (22)$$

For the special case of only considering MC, polarization angles are $\Phi_t^1/\Phi_t^2 = 0°/0°$ and $\Phi_r^1/\Phi_r^2 = 0°/0°$. The 2×2 channel matrix with MC can be rewritten as

$$[\mathbf{H}^c]_{2\times 2} = \iint_{(\phi_r,\phi_t)} \left\{ e^{j2\pi f_c t} e^{j2\pi f_d t} p(\phi_r) p(\phi_t) \right\} \odot \begin{bmatrix} G_{11} & G_{12} \\ G_{21} & G_{22} \end{bmatrix} d\phi_t d\phi_r \tag{23}$$

where

$$\begin{aligned} G_{11} &= e^{j\varphi^{VV}} \left\{ C_r^{11} C_t^{11} + C_r^{12} C_t^{11} e^{j\tau_r} + C_r^{11} C_t^{21} e^{j\tau_t} + C_r^{12} C_t^{21} e^{j(\tau_r+\tau_t)} \right\} \\ G_{12} &= e^{j\varphi^{VV}} \left\{ C_r^{11} C_t^{12} + C_r^{12} C_t^{12} e^{j\tau_r} + C_r^{11} C_t^{22} e^{j\tau_t} + C_r^{12} C_t^{22} e^{j(\tau_r+\tau_t)} \right\} \\ G_{21} &= e^{j\varphi^{VV}} \left\{ C_r^{21} C_t^{11} + C_r^{22} C_t^{11} e^{j\tau_r} + C_r^{21} C_t^{21} e^{j\tau_t} + C_r^{22} C_t^{21} e^{j(\tau_r+\tau_t)} \right\} \\ G_{22} &= e^{j\varphi^{VV}} \left\{ C_r^{21} C_t^{12} + C_r^{22} C_t^{12} e^{j\tau_r} + C_r^{21} C_t^{22} e^{j\tau_t} + C_r^{22} C_t^{22} e^{j(\tau_r+\tau_t)} \right\} \end{aligned} \tag{24}$$

here, $\tau_t = 2\pi d/\lambda \sin\phi_t$, $\tau_r = 2\pi d/\lambda \sin\phi_r$. Similarly, if we only consider polarization which makes mutual impedances Z_{12} and Z_{21} equal to 0, MC matrix can be simplified as the unit matrix. Submitting $\Phi_t^1/\Phi_t^2 = 45°/-45°$, $\Phi_r^1/\Phi_r^2 = 0°/90°$ to (22), the 2×2 channel matrix with polarization can be rewritten as

$$\begin{aligned} [\mathbf{H}^p]_{2\times 2} \;=\; & \iint_{(\phi_r,\phi_t)} \left\{ e^{j2\pi f_c t} e^{j2\pi f_d t} p(\phi_r) p(\phi_t) \right\} \\ & \odot \begin{bmatrix} \dfrac{\sqrt{2}(h_{VV} + h_{HV}\cos\phi_t)}{2} & \dfrac{\sqrt{2}e^{j\tau_t}(h_{VV} - h_{HV}\cos\phi_t)}{2} \\ \dfrac{\sqrt{2}e^{j\tau_r}\cos\phi_r(h_{VH} + h_{HH}\cos\phi_t)}{2} & \dfrac{\sqrt{2}e^{j(\tau_t+\tau_t)}\cos\phi_r(h_{VH} - h_{HH}\cos\phi_t)}{2} \end{bmatrix} d\phi_t d\phi_r \end{aligned} \tag{25}$$

4.2. Cross-Correlation

We apply our new model on the propagation scene of suburban macro cellular given by 3 GPP SCM channel standard, where both AoA and AoD include six clusters, and each cluster follows Laplace distributions, which is observed in many measurement tests [17] and can be expressed as

$$p(\phi_r) = \frac{1}{\left(1 - e^{-\sqrt{2}\pi/2\sigma}\right)\sqrt{2}\sigma} e^{-\sqrt{2}|\phi_r - \phi_r^0|/\sigma}, \quad |\phi_r - \phi_r^0| \le \frac{\pi}{2} \tag{26}$$

Here Φ_r^0 and σ denote average value and angle spread. As one trial, the simulation parameter of XPD is 8 dB, angle spread and average angle for AoA are 35° and [63.2°; 100.4°; 79.4°; 9.4°; 50.0°; −23.5°], and the counterpart of AoD are 2° and [30.4°; 30.7°; 31.2°; 25.7°; 34.4°; 38.9°].

Figure 9 gives the simulation results of spatial correlation between different sub-channels of MIMO channel, where the value of correlation represents the statistical average on six clusters. Fig. 9(a) shows that for the case of double transmitters and single receiver channel ($\Phi_t^1/\Phi_r^1 = 45°/0°$, $\Phi_t^2/\Phi_r^1 = -45°/0°$), correlation curve with MC shocks around the curve of no coupling, and correlation with polarization is slightly less than the correlation without polarization.

Similarly, Fig. 9(b)–Fig. 9(d) show that for the cases of double receivers and single transmitter channel ($\Phi_t^1/\Phi_r^1 = 45°/0°$, $\Phi_t^1/\Phi_r^2 = 45°/90°$), parallel channel ($\Phi_t^1/\Phi_r^1 = 45°/0°$, $\Phi_t^2/\Phi_r^2 = -45°/90°$) and cross channel ($\Phi_t^1/\Phi_r^2 = 45°/90°$, $\Phi_t^2/\Phi_r^1 = -45°/0°$), cross-correlation curve with MC decreases compared with that without coupling, correlation curve with polarization also decreases for different polarization combinations. Thus, the curve combining MC with polarization decreases compared with that without coupling and polarization. Moreover, when the distance is long enough, the effect of coupling is very slight.

4.3. Channel Capacity

Ergodic capacity of MIMO channel with the strategy of uniformly distributed transmitting power is an important performance parameter for communication system and defined as

$$\bar{C} = \mathrm{E}_{\mathbf{H}}\left[\log_2 \det\left(\mathbf{I}_{N_r} + \frac{\zeta}{N_t}\mathbf{H}^{p,c}(\mathbf{H}^{p,c})^H\right)\right] \tag{27}$$

where ζ is the average signal-to-noise ratio (SNR) and $\mathbf{I}$ the identity matrix. To investigate the characteristics of $\mathbf{H}^{p,c}$, we can perform an SVD of $\mathbf{H}^{p,c}$ to diagonalize $\mathbf{H}^{p,c}$ and determine the eigenvalues. The SVD expansion of matrix $\mathbf{H}^{p,c}$ can be expressed by

$$\mathbf{H} = \mathbf{U}\mathbf{\Lambda}\mathbf{V}^H \tag{28}$$

where $\mathbf{U}$ and $\mathbf{V}$ are unitary matrices, and $\mathbf{\Lambda}$ is nonnegative and diagonal with entries specified by

$$\mathbf{\Lambda} = \mathrm{diag}\left(\sqrt{\lambda_1}, \sqrt{\lambda_2}, \ldots, \sqrt{\lambda_q}, 0, \ldots, 0\right) \tag{29}$$

where $\lambda_1, \lambda_2, \ldots, \lambda_q$ are the nonzero eigenvalues of $\mathbf{H}^{p,c}(\mathbf{H}^{p,c})^H$ or $(\mathbf{H}^{p,c})^H\mathbf{H}^{p,c}$. The SVD shows that the channel matrix $\mathbf{H}^{p,c}$ can be diagonalized to a number of independent orthogonal sub-channels, where

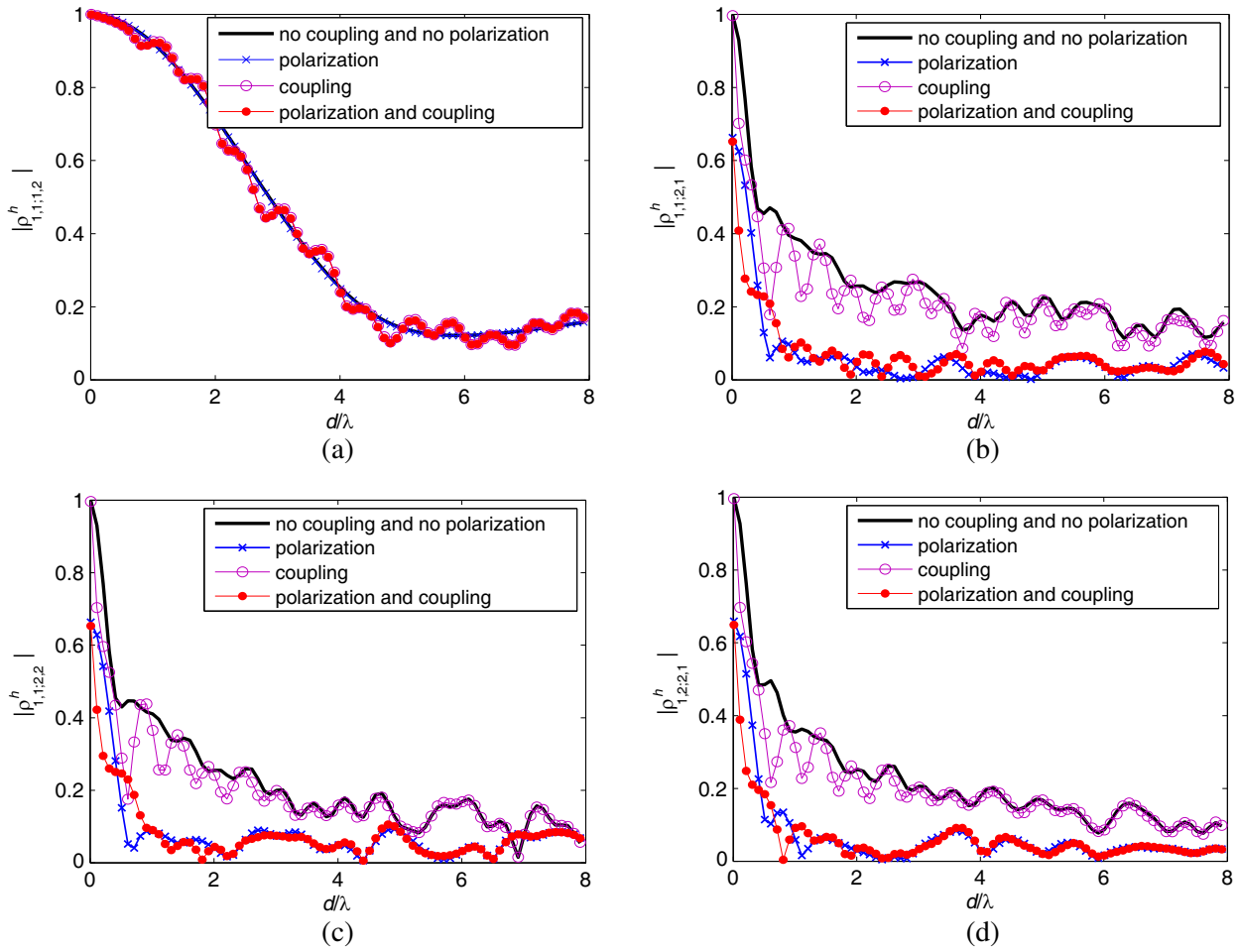

Figure 9. Cross-correlation comparison versus normalized antenna spacing. (a) Double transmitters and single receiver. (b) Double receivers and single transmitter. (c) Parallel channel. (d) Cross channel.

the power gain of the ith channel is λ_i. Thus, (27) can be rewritten as

$$\bar{C} = E\left\{\sum_{i=1}^{q} \log_2\left(1 + (\zeta/N_t)\lambda_i\right)\right\} \tag{30}$$

Making use of Eq. (30) on our new model, we can get the channel capacity incorporating polarization and MC. Capacity curves versus SNR with $d/\lambda = 0.1$ and $d/\lambda = 0.5$ are given in Fig. 10, which shows that independent channel $\mathbf{H}_{iid}$ has the best capacity than other cases. For the case of MC, channel capacity is smaller than that without coupling and polarization. Moreover, the capacity loss decreases when antenna space increases. As we see, the difference is very small as $d/\lambda = 0.1$, which means the effect of MC can be ignored in this case. For the case of polarization, the results are more complicated. When SNR is greater than 20 dB and $d/\lambda = 0.1$, channel capacity with polarization is more than that without polarization and coupling, which is counter to that under low SNR. The main reason is polarization antenna will reduce the channel correlation, while depolarization will lead to signal power loss. In other words, the contributions to channel capacity of polarization and depolarization are opposite. When polarization and MC are both considered, capacity is less than that without polarization and MC.

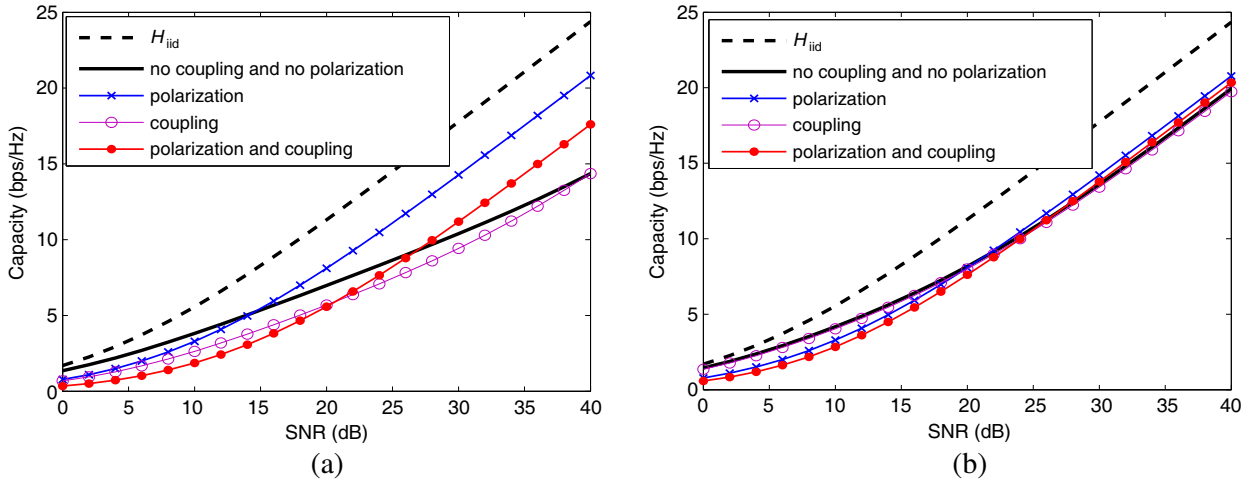

Figure 10. Capacity comparison versus SNR. (a) $d/\lambda = 0.1$, (b) $d/\lambda = 0.5$.

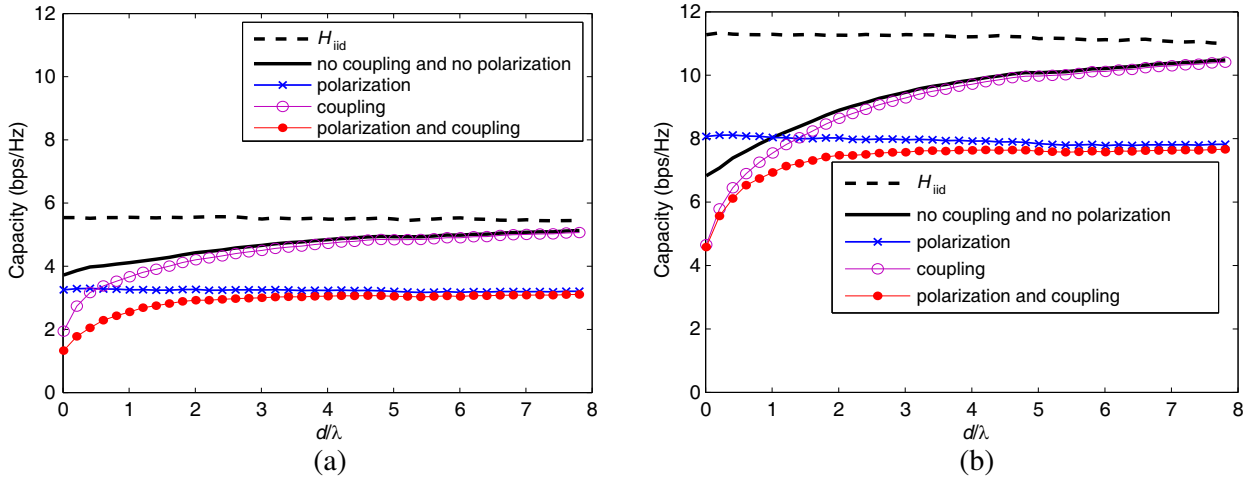

Figure 11. Capacity comparison versus normalized antenna spacing. (a) SNR = 10 dB, (b) SNR = 20 dB.

Moreover, the capacity with long spacing is more than that with short spacing. Finally, the capacities of all cases increase with the increasing of SNR.

Figure 11 gives the relationship between capacity and antenna space when SNR is 10 dB and 20 dB. As we can see, capacity of independent channel is the largest one and does not change for different spaces. When MC is considered, capacity is less than that without coupling, and the difference becomes tiny as $d/\lambda \geq 4$. If we consider antenna polarization, when SNR is low, capacity is less than that without polarization. Moreover, when SNR is large, capacity is more than that without polarization at small distance, which verifies the results in Fig. 10. Considering both polarization and MC, capacity increases with the distance, but it is smaller than that without polarization and coupling. In addition, when d/λ is large, the effect of MC is little, and capacity curve approaches the curve of polarization.

5. CONCLUSION

In this paper, we develop a new MIMO channel model incorporating antenna effects based on the clustered model. Our model accounts for antenna effects like element spacing, pattern, polarization/depolarization and MC, as well as path loss, scattering and fading. At the same time, we analyze the effects of MC and polarization/depolarization on signal vector, signal power and signal correlation in detail, and derive their close-form expressions respectively. Analysis results show that MC and polarization/depolarization will not only reduce cross-correlation but also reduce the power of receiving signal. Finally, we apply our model to a 2×2 MIMO system under the propagation scene of suburban macro cellular to verify the effects caused by polarization/depolarization and MC, which has great significance in improving the performance of MIMO system.

ACKNOWLEDGMENT

This work is supported by the Fundamental Research Funds for the Central Universities (NS2015046, NS2016044), Foundation of Jiangsu Key Laboratory of Internet of Things and Control Technologies (NJ20160027).

REFERENCES

1. Shi, D. S., G. J. Foschini, and M. J. Gans, "Fading correlation and its effect on the capacity of multi-element antenna systems," *IEEE Transactions on Communications*, Vol. 48, No. 3, 502–513, 2000.
2. Lau, B. K. and J. B. Andersen, "Simple and efficient decoupling of compact arrays with parasitic scatterers," *IEEE Transactions on Antennas and Propagation*, Vol. 60, No. 2, 464–472, 2012.
3. Masouros, C., M. Sellathurai, and T. Ratnarajah, "Large-scale MIMO transmitters in fixed physical spaces: The effect of transmit correlation and mutual coupling," *IEEE Transactions on Communications*, Vol. 61, No. 7, 2794–2804, 2013.
4. Wu, Y., J. W. M. Bergmans, and S. Attallah, "Effects of antenna correlation and mutual coupling on the carrier frequency offset estimation in MIMO systems," *IEEE Conference on Wireless Communications Networking and Mobile Computing (WiCOM)*, 1–4, 2010.
5. Abouda, A. A. and S. G. Häggman, "Effect of mutual coupling on capacity of MIMO wireless channels in high SNR scenario," *Progress In Electromagnetics Research*, Vol. 65, 27–40, 2006.
6. Gesbert, D., M. Shafi, and D. Shiu, "From theory to practice: An overview of MIMO space-time coded wireless systems," *IEEE Journal on Selected Areas in Communications*, Vol. 21, No. 3, 281–302, 2003.
7. Varzakas, P., "Average channel capacity for Rayleigh fading spread spectrum MIMO systems," *International Journal of Communication Systems*, Vol. 19, No. 10, 1081–1087, 2006.
8. Valenzuela-Valdes, J. F., M. Garcia-Fernandez, A. M. Martinez-Gonzalez, et al., "Evaluation of true polarization diversity for MIMO systems," *Ophthalmic Surgery*, Vol. 25, No. 10, 690–694, 2009.

9. Huang, L. Q. and Y. W. Guo, "Channel capacity of MIMO wireless systems in the presence of prolarization diversity," *Journal of Electronics & Information Technology*, Vol. 28, No. 8, 1443–1446, 2006.
10. Shafi, M., M. Zhang, and A. L. Moustakas, "Polarized MIMO channels in 3-D: Models, measurements and mutual information," *IEEE Journal on Selected Areas in Communications*, Vol. 24, No. 3, 514–527, 2006.
11. Dao, M. T., V. A. Nguyen, and Y. T. Im, "3D polarized channel modeling and performance comparison of MIMO antenna configurations with different polarizations," *IEEE Transactions on Antennas and Propagation*, Vol. 59, No. 7, 2672–2682, 2011.
12. Lu, W., Y. Liu, and D. Wang, "Capacity performance of polarized distributed MIMO system on Rician channel," *Wireless Personal Communications*, Vol. 68, No. 3, 1047–1066, 2013.
13. Joung, H., H.-S. Jo, C. Mun, and J.-G. Yook, "Capacity loss due to polarization-mismatch and space-correlation on MISO channel," *IEEE Transactions on Wireless Communications*, Vol. 13, No. 4, 2124–2136, 2014.
14. Clerckx, B., C. Craeye, D. Vanhoenacker-Janvier, et al., "Impact of antenna coupling on 2×2 MIMO communications," *IEEE Transactions on Vehicular Technology*, Vol. 56, No. 3, 1009–1018, 2007.
15. Zhao, J., Y. Li, and G. Sun, "Analysis of antenna mutual coupling in the X-type polarization diversity system," *IEEE Conference on Wireless Communications*, 1–4, 2009.
16. Wu, S., C. X. Wang, and E. H. M. Aggoune, "A non-stationary 3-D wideband twin-cluster model for 5G massive MIMO channels," *IEEE Journal on Selected Areas in Communications*, Vol. 32, No. 6, 1207–1218, 2014.
17. Zhang, J. H., C. Pan, and F. Pei, "Three-dimensional fading channel models: A survey of elevation angle research," *IEEE Communications Magazine*, Vol. 52, No. 6, 218–226, 2014.